ChemComm

COMMUNICATION

View Article Online
View Journal | View Issue

Cite this: *Chem. Commun.*, 2017, 53, 4620

Received 14th February 2017, Accepted 28th March 2017

DOI: 10.1039/c7cc00540g

rsc.li/chemcomm

A combination strategy using two novel cerium-based nanocomposite affinity probes for the selective enrichment of mono- and multi-phosphopeptides in mass spectrometric analysis†

Xing-yu Long,[ab] Zi-jin Zhang,[a] Jia-yuan Li,[a] Dong Sheng[a] and Hong-zhen Lian *[a]

This work presents a sequential enrichment protocol, based on two self-designed cerium-based nanocomposite affinity probes, which not only can effectively separate phosphopeptides from non-phosphopeptides but can also selectively differentiate mono- and multi-phosphopeptides for direct matrix-assisted laser desorption/ionization time-of-flight mass spectrometric (MALDI-TOF MS) analysis.

Multisite phosphorylation is a very ubiquitous occurrence. However, the different levels of phosphorylation (mono-/multi-site phosphorylation) can reveal the diversity of the functions of versatile post translational modification (PTM). For example, activation of the epidermal growth factor (EGF) receptor indicates that the phosphorylation of multiple tyrosine residues is caused by another EGF receptor, which indicates that multiple phosphorylation acts as a device function.[1] In addition, mono- and multisite phosphorylation of B-cell lymphoma-2 (Bcl-2) either enhances its antiapoptotic function or inactivates Bcl-2.[2] However, the mechanism of phosphorylation of Bcl-2, which determines how its survival function and cell cycle retardation are regulated, together with the distributions of monosite and/or multisite phosphorylation, is still not yet clear. Therefore, it is of prime importance to develop new methods that can not only isolate phosphopeptides from complicated samples, but can also differentiate the levels of phosphorylation with a high resolution.[3]

Currently, mass spectrometry (MS) is a robust tool which has been widely employed for the analysis of phosphorylation sites. However, the signals of phosphopeptides are frequently suppressed by abundant non-phosphopeptides, and there are inherent short-comings such as low stoichiometry and difficulty of ionization. In particular, when using common electrospray ionization mass spectrometry (ESI-MS) in positive ion mode, the signal response of phosphopeptides is far from desirable because of the strongly negatively charged phosphate group.[4] To make things worse, some multi-phosphorylated peptides (which have more phosphate groups) cannot even be detected. Matrix-assisted laser desorption/ionization time-of-flight mass spectrometry (MALDI-TOF MS) is an effective and sensitive analytical technique which is extensively used to analyse the phosphorylation sites. Nevertheless, it is undeniable that there are still some problems relating to the inhibition of multi-phosphopeptides.[5] Overall, owing to the low abundance and ionization efficiency of phosphorylated proteins/peptides and the signal suppression by non-phosphopeptides in MS, the strategy for comprehensive identification and recognition of the phosphorylated sites in proteins is still a challenge.[6] Therefore, it is necessary to develop new methods for selectively enriching and effectively extracting phosphopeptides, especially multi-phosphopeptides, from non-phosphopeptides prior to MS analysis.

Recently, many strategies, including metal oxide affinity chromatography (MOAC)[7] and immobilized metal ion affinity chromatography (IMAC),[8] which are the most commonly used methods, have been developed for phosphopeptide enrichment research. Despite recent advances in phosphopeptide research, dissection of the levels of phosphorylation, as well as the respective characterization and detection of mono- or multi-phosphorylated peptides, has been a huge challenge. Most of the above-mentioned methods tend to exhibit excellently preferential detection for mono-phosphorylated peptides, thus easily leading to the exclusion of valuable information closely relevant to the multi-phosphopeptides.[9] Accordingly, it is essential and logical to devise novel strategies and develop new materials for the preferential isolation of multi-phosphopeptides as well as the effective retention of mono-phosphopeptides. To date, only a few papers have reported on the specific analysis of multi-phosphorylated peptides.[10] In addition, Bai and Liu's group has successfully developed guanidyl-functionalized graphene[11] and hydrazide-functionalized monodispersed silica microspheres[12] as novel materials for the enrichment of global phosphopeptides,

[a] *State Key Laboratory of Analytical Chemistry for Life Science, Collaborative Innovation Center of Chemistry for Life Sciences, School of Chemistry & Chemical Engineering and Center of Materials Analysis, Nanjing University, 163 Xianlin Avenue, Nanjing 210023, P. R. China. E-mail: hzlian@nju.edu.cn; Tel: +86 25 8368 6075*

[b] *Editorial Department of Journal, Guizhou Normal University, 180 Baoshan North Road, Guiyang 550001, P. R. China*

† Electronic supplementary information (ESI) available. See DOI: 10.1039/c7cc00540g

multi-phosphopeptides only, or different-level phosphopeptides, by simple modulation of the loading buffer. Also, guanidyl was introduced onto a poly(glycidyl methacrylate)-modified Fe_3O_4 microsphere by Zou's group which resulted in similar properties.[13] Although Larsen and his team[14] achieved the rapid separation of mono-phosphorylated peptides from multi-phosphorylated peptides using the phosphoproteomics strategy with the sequential elution from IMAC, to the best of our knowledge, no prior work has been reported for the simultaneous analysis of mono- and multi-phosphopeptides.

In the present study, we developed two novel cerium-based nanocomposites for the first time: PEG-modified magnetic nano-cerium/cerium(IV) oxide particles (denoted as PEG–Ce/CeO_2–Fe_3O_4, P-CCF), and Ce/CeO_2 doped SO_4^{2-}/Fe_2O_3 (denoted as Ce/CeO_2–SO_4^{2-}/Fe_2O_3, CSF) nanosolid superacid (NS) affinity probes. Moreover, after thorough characterization, these two materials were utilised as affinity probes for the selective enrichment and effective isolation of mono- and/or multi-phosphopeptides with combined strategies. In detail, through different sequential enrichment processes, the flowthrough fractions from P-CCF and CSF were inversely enriched by each other, which provided a comprehensive way to analyse global phosphopeptides. The NS CSF probe exhibited a high specific selectivity for multi-phosphopeptides, while the mono-phosphopeptides remaining in the effluent passing through CSF were further extracted with P-CCF. In this way, the effective stepwise enrichment of mono- and multi-phosphopeptides was achieved successfully.

As illustrated in Scheme S1 in the ESI,† the P-CCF and CSF affinity probes were synthesized *via* co-precipitation and solvothermal methods respectively. It should be noted that both the co-precipitation and solvothermal methods failed to form the cerium spinel structure in our pilot experiment. For P-CCF, according to the standard electrode potential ($\varphi_{Ce^{4+}/Ce^{3+}} = 1.61$ V; $\varphi_{Fe^{3+}/Fe^{2+}} = 0.771$ V), as a strong oxidant, Ce^{4+} can partially oxidize Fe^{2+} to Fe^{3+} under acidic conditions ($Ce^{4+} + Fe^{2+} = Fe^{3+} + Ce^{3+}$). Following this, adjusting the pH to 12–13 with $NH_3{\cdot}H_2O$ caused the numerous magnetic metal oxides to co-precipitate, including CeO_2 and Fe_3O_4 with the particle-to-particle being wreathed by PEG, which is dissimilar to the formation of the corresponding spinels of the metal ions in this situation, such as Ni^+, Zn^{2+}, Mn^{2+}, Cu^{2+}, Co^{2+} and so on.[3c,15] It is likely that the surface bonding energy of Ce^{4+} or Ce^{3+} is higher than that of other metal ions.[16] As for CSF, the system of Fe^{3+}–EG–NaAc is a classical solvothermal method with EG as a reductant for preparing magnetic Fe_3O_4.[17] When Ce^{4+} was introduced, it was expected that cerium spinel would form, just like with Mn^{2+}.[18] However, the ability of Ce^{4+} to oxidize Fe^{2+} is much stronger than that of EG to reduce Fe^{3+}, which resulted in a shortage of Fe^{2+}, causing the formation of Fe_3O_4 to fail, and forming Fe_2O_3 instead. In addition, Ce^{4+} was dissolved in a sulphuric acid solution in this experiment, and Fe_2O_3 has a tendency to form NS (SO_4^{2-}/Fe_2O_3) when dissolved in H_2SO_4 at high temperature and pressure.[19] Moreover, the initial off white cerium oxide (Ce_2O_3) product soon became CeO_2 under air-oxidation, and the final light peachblow cerium(IV) sulfate adhered to SO_4^{2-}/Fe_2O_3. In summary, the P-CCF and CSF affinity probes were respectively prepared by different processes.

As is well known, metal oxides (CeO_2, Fe_3O_4 and Fe_2O_3) are commonly used as adsorbents for phosphopeptide enrichment.[3c,20] Therefore, the two self-designed Ce-based nanocomposites have the potential to be innovatively utilized for the isolation and enrichment of phosphopeptides. Furthermore, the acidity of NS is even stronger than 100% sulfuric acid,[19a] and it endows the strong surface activity with more positive charges, thus the CSF probe with its unique selectivity favours the selective capture of multi-phosphopeptides (which have more negative charges) and effectively excludes mono-phosphopeptides. In addition, CeO_2 acts as a catalyst for dephosphorylation in the identification of phosphopeptides. The CSF probe material is used to trap multi-phosphopeptides, while the P-CCF probe material assists in the capture of mono-phosphopeptides. In addition, both of these materials can catalyse dephosphorylation.

The characterization of P-CCF and CSF probes was carried out by FT-IR, EDX, SEM, TEM and XRD. The FT-IR results (Fig. S1A, ESI†) were in good accordance with the EDX analysis (Fig. S1B and C, ESI†), *i.e.* both P-CCF and CSF were composed of the same common elements, O, Fe and Ce, except for the characteristic element of C for P-CCF, and S for CSF. TEM, HRTEM and SEM images of P-CCF and CSF are shown in Fig. S2A–D and E–H respectively in ESI.† It is further confirmed that the polycrystalline structure of P-CCF consists of various Fe_3O_4 nanocrystallites and mischcrystals (CeO_2, Ce and Fe_2O_3 nanocrystallites), while the polycrystalline structure of CSF is also composed of numerous mischcrystals (Fe_2O_3, CeO_2 and Ce nanocrystallites). Based on the analysis of the XRD patterns of P-CCF and CSF (Fig. S3 in ESI†), the components and crystal structures of the P-CCF and CSF nanocomposites were further elucidated. In addition, the magnetic properties of P-CCF were examined using a Superconducting Quantum Interference Device (SQUID). Such a high saturation magnetization value (43.1 emu g^{-1}) enabled the convenient magnetic separation of P-CCF (Fig. S4 in ESI†). These two novel Ce-based metal oxide nanocomposites are ideal affinity materials for phosphopeptide enrichment due to the intense interactions between their positively charged metal oxide surface (Fe^{3+} and Ce^{4+}) and the negatively charged phosphate groups, as well as their ability to catalyse dephosphorylation (doped by CeO_2).[20a]

To evaluate the efficiency of the two Ce-based nanocomposites for selectively capturing mono-/multi-phosphopeptides, a mixture of standard phosphoprotein (10 pmol, α-/β-casein, v/v = 1 : 1) tryptic digests was used as a model. The enrichment protocol (Scheme 1) was conducted on P-CCF and CSF probes under the same conditions (Experimental section in the ESI†). Two serial enrichment strategies (step I and II) for the flowthrough fractions of P-CCF and CSF were inversely enriched by each other. Only 5 weak phosphopeptide peaks (marked with "*", including 4 mono- and 1 multi-phosphopeptide peaks) appeared in the mass spectrum before enrichment (Fig. 1a). After enrichment of the original samples for step I, the results showed that CSF had a preference for multi-phosphopeptides (marked with "*", Fig. 1b) whereas the response to mono-phosphopeptides

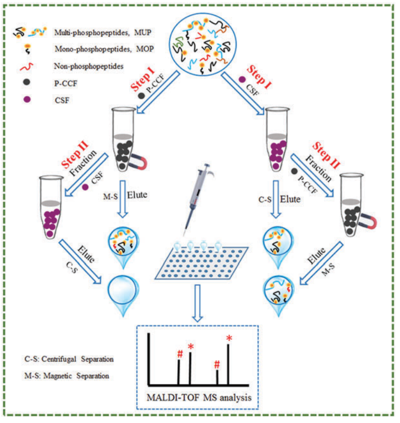

Scheme 1 Experimental protocol. Two serial phosphopeptide enrichment strategies (step I and II) for the flowthrough fractions of P-CCF and CSF are inversely enriched by each other.

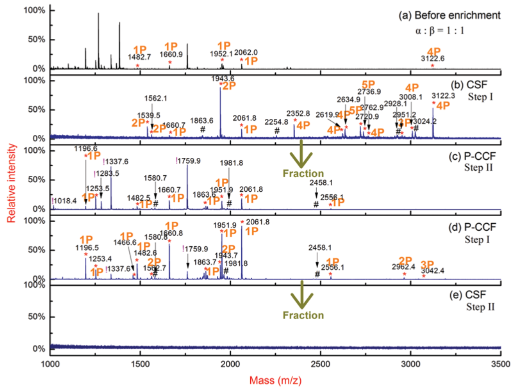

Fig. 1 MALDI-TOF mass spectra of two serial enrichment strategies (step I and II): before enrichment (a); step I: direct enrichment from the tryptic digests of α-/β-casein (10 pmol, v/v = 1 : 1) with CSF (b) and P-CCF (d); step II: from the flowthrough fraction of CSF treated with P-CCF (c) and that of P-CCF treated with CSF (e). Phosphorylations were labelled as P. The Arabic numeral before P represents mono-/multi-phosphopeptides. Mass spectrometric peaks are marked as: phosphopeptides (*), dephosphorylated fragment (#), and non-phosphopeptides or unknown impurities (!).

(*m/z* 1660.7, 2061.8, 1P) was very low. Using P-CCF, some mono-/multi-phosphopeptides were detected with a strong intensity, as well as two non-phosphopeptides with a low intensity (*m/z* 1337.6 and 1759.9, marked with "!", Fig. 1d). For step II, in the corresponding fractions from step I using a P-CCF probe, most of the detected phosphopeptides were mono-phosphopeptides (marked with "*"), together with 4 non-phosphopeptides or unknown impurities (*m/z* 1018.4, 1283.5, 1337.6 and 1759.9, marked with "!", Fig. 1c). When the corresponding fractions were treated with CSF, no peptides were detected (Fig. 1e). In addition, the series of fragment peaks (*m/z* 1580.7, 1863.6, 1981.8, 2458.1, 2928.1, and 3024.2, marked with "#") arose from dephosphorylation through the loss of HPO_3 (80 Da) from the corresponding phosphopeptides (*m/z* 1660.7, 1943.6, 2061.8, 2556.1, 3008.1, and 3122.3), respectively. The identified mono-/multi-phosphopeptides enriched by the CSF and P-CCF probes in the amino acid sequence pattern are listed in Table S1 in the ESI.† These results reveal the following. (1) Overall, the capture of phosphopeptides is due to affinity interactions between the metal ions (Fe^{3+} and Ce^{4+}) of P-CCF/CSF and the phosphate groups of the phosphopeptides. (2) The CSF probe has special selectivity towards multi-phosphopeptides and excludes mono-phosphopeptides, due to its superacid properties and high activity. The surface of CSF is abundant with positive charges which can interact with the multi-phosphorylated peptides, which have more negative charges. In detail, the adsorption of multi-phosphopeptides by CSF is attributed to the strong electrostatic interactions occurring between the nanosolid superacid (NS) and the multiple phosphate groups (nP, $n > 1$) to form [NS](+)(+)···[nP](−)(−), rather than that with the mono-phosphate group to form [NS](+)(+)···[1P](−). (3) The global phosphopeptides can be extracted by P-CCF (no multi-phosphopeptide was extracted from the fraction of P-CCF treatment by CSF). The powerful peptide adsorbability of P-CCF gives it an advantage over CSF, which is likely due to the hydrophobicity of the carbon chains introduced by PEG. (4) The occurrence of dephosphorylated fragment peaks confirms that the two doped-CeO_2 affinity probes are excellent catalysts for the dephosphorylation process. Therefore, the application of P-CCF as an absorbent is a simple alternative method for the relatively comprehensive analysis of phosphopeptides. More interestingly, the proposed sequential enrichment by CSF and P-CCF would provide a promising strategy to effectively separate phosphopeptides from non-phosphopeptides, and selectively differentiate mono- and multi-phosphopeptides.

The limit of detection and the selectivity for phosphopeptide enrichment of these two affinity probes were evaluated as described in Part 1 of the ESI.† The sequential enrichment with two Ce-based nanocomposites was applied to capture phosphopeptides from the tryptic digest of non-fat milk. Only 3 phosphopeptides (containing 2 mono-phosphopeptides and 1 multi-phosphopeptide) with low intensity were detected without enrichment (Fig. S8a, ESI†). After CSF enrichment (step I), 7 multi-phosphopeptides and one mono-phosphopeptide (*m/z* 2061.8, 1P) were detected (Fig. S8b, ESI†), while 12 phosphopeptides were obtained after P-CCF enrichment including 8 mono-phosphopeptides and 4 multi-phosphopeptides, together with 4 non-phosphopeptides or unknown impurity peaks (*m/z* 1065.5, 1245.5, 1759.9 and 2313.2, marked with "!", Fig. S8d, ESI†). For step II, inversely extracting from the fractions, by adopting the second step of enrichment and using P-CCF, it was found that most of the detected phosphopeptides were mono-phosphopeptides (marked with "*") together with 3 non-phosphopeptides (*m/z* 1245.5, 1759.9 and 2313.2, marked with "!", Fig. S8c, ESI†). However, no peptides were detected with CSF (Fig. S8e in the ESI†). Overall, CSF exhibited preferential enrichment for multi-phosphopeptides and P-CCF complementally trapped mono-phosphopeptides from the rest of the fractions of CSF. All mono-/multi-phosphopeptides identified in the analyses are shown in Table S2 in the ESI.† In addition, human serum was employed as a real-world biological sample to further investigate the performance of these two Ce-based nanocomposite probes with a combined strategy for the selective capture of mono- and/or multi-phosphopeptides.

Only one weak mono-phosphopeptide peak (*m*/*z* 1616.8, 1P) was detected before enrichment (Fig. S9a in the ESI†). For step I, after enrichment with CSF, no multi-phosphopeptides were obtained (Fig. S9b in the ESI†), while with P-CCF, 4 mono-phosphopeptides (*m*/*z* 1389.5, 1460.5, 1545.5 and 1616.6, marked with "*", 1P, their amino acid sequences are listed in Table S3 in the ESI†) were obtained and identified in the mass spectrum (Fig. S9d in the ESI†). There are not likely to be any multi-phosphopeptides in the original human serum sample in the low molecular weight range of 1000–3500 Da.[21] For step II, after serial enrichment from the fractions of CSF with P-CCF, the same four mono-phosphopeptides (marked with "*") and some of the dephosphorylated fragments (*m*/*z* 1380.7, 1465.6, 1536.6, marked with "#") were detected (Fig. S9c in the ESI†). Noticeably, the phosphopeptide (*m*/*z* 1493.2, 1P), which can be recognized from the loss of 98 Da through MALDI tandem mass spectrometry (MS/MS) (Fig. S10 in the ESI†), was also obtained with a good signal response, whereas it could be lost by direct treatment with P-CCF or CSF. As expected, these results further indicate that the CSF probe possesses the capability to extract only multi-phosphorylated peptides and retain mono-phosphopeptides in the rest of the fractions. Serial enrichment, which consists of the methods with CSF for step I and P-CCF for step II, can provide a good protocol for global phosphopeptide enrichment. Additionally, similar properties of the two affinity probes were observed with the same combined strategies of enriching mono-/multi-phosphopeptides from the serum samples that were spiked with α-casein tryptic digests (Fig. S11 in the ESI†).

In conclusion, we have for the first time designed and prepared two diverse Ce-based nanocomposite probes (P-CCF and CSF). The sequential enrichment using these two affinity probes was applied to the highly selective enrichment of phosphopeptides from digests of a mixture of standard proteins (α-/β-casein, v/v = 1 : 1) and a practical sample (non-fat milk), as well as a biological sample (human serum). The proposed enrichment strategy can not only effectively separate phosphopeptides from non-phosphopeptides, but can also distinguish mono- and multi-phosphopeptides. Concretely, the CSF probe is used to trap multi-phosphopeptides, while the P-CCF probe assists in the capture of mono-phosphopeptides. In this way, the effective step-wise enrichment of mono- and multi-phosphopeptides is achieved successfully, and thus can provide a good alternative for global phosphopeptide enrichment. In addition, these two CeO_2-doped affinity probes exhibit the property of dephosphorylation catalysis. Therefore, our experimental results will be helpful to collect crucial complementary information from mono- and multi-phosphopeptides, which may provide a comprehensive understanding of the essential biological phosphorylation processes in modern life science.

This work was supported by the National Natural Science Foundation of China (21275069, 21577057, 91643105), and the Analysis & Test Fund of Nanjing University.

Notes and references

1 T. Pawson and P. Nash, *Genes Dev.*, 2000, **14**, 1027.
2 X. Deng, F. Gao, T. Flagg and W. S. May Jr., *Proc. Natl. Acad. Sci. U. S. A.*, 2004, **101**, 153.
3 (*a*) C. Chan, X. Liu, L. Wang, L. Bardwell, Q. Nie and G. Enciso, *PLoS Comput. Biol.*, 2012, **8**, e1002551; (*b*) P. Cohen, *Trends Biochem. Sci.*, 2000, **25**, 596; (*c*) H. Zhong, X. Xiao, S. Zheng, W. Zhang, M. Ding, H. Jiang, L. Huang and J. Kang, *Nat. Commun.*, 2013, **4**, 1656.
4 H. Wan, J. Yan, L. Yu, X. Zhang, X. Xue, X. Li and X. Liang, *Talanta*, 2010, **82**, 1701.
5 (*a*) R. Ma, J. Hu, Z. Cai and H. Ju, *Talanta*, 2014, **119**, 452; (*b*) J. Wei, Y. Zhang, J. Wang, F. Tan, J. Liu, Y. Cai and X. Qian, *Rapid Commun. Mass Spectrom.*, 2008, **22**, 1069.
6 Z.-G. Wang, N. Lv, W.-Z. Bi, J.-L. Zhang and J.-Z. Ni, *ACS Appl. Mater. Interfaces*, 2015, **7**, 8377.
7 (*a*) G. Cheng, Z.-G. Wang, Y.-L. Liu, J.-L. Zhang, D.-H. Sun and J.-Z. Ni, *ACS Appl. Mater. Interfaces*, 2013, **5**, 3182; (*b*) X. Qi, L. Chen, C. Zhang, X. Xu, Y. Zhang, Y. Bai and H. Liu, *ACS Appl. Mater. Interfaces*, 2016, **8**, 18675; (*c*) F. Jabeen, M. Najam-ul-Haq, M. Rainer, Y. Güzel, C. W. Huck and G. K. Bonn, *Anal. Chem.*, 2015, **87**, 4726.
8 (*a*) M. Zhao, C. Deng and X. Zhang, *Chem. Commun.*, 2014, **50**, 6228; (*b*) Y. Yan, Z. Zheng, C. Deng, Y. Li, X. Zhang and P. Yang, *Anal. Chem.*, 2013, **85**, 8483.
9 (*a*) L. Qiao, H. Bi, J.-M. Busnel, M. Hojeij, M. Mendez, B. Liu and H. H. Girault, *Chem. Sci.*, 2010, **1**, 374; (*b*) J. Wan, K. Qian, L. Qiao, Y. Wang, J. Kong, P. Yang, B. Liu and C. Yu, *Chem. – Eur. J.*, 2009, **15**, 2504.
10 (*a*) J. Kim, D. G. Camp II and R. D. Smith, *J. Mass Spectrom.*, 2004, **39**, 208; (*b*) S. Kim, H. Choi and Z.-Y. Park, *Mol. Cells*, 2007, **23**, 340; (*c*) H. Wang, J. Duan, L. Zhang, Z. Liang, W. Zhang and Y. Zhang, *J. Sep. Sci.*, 2008, **31**, 480.
11 L.-N. Xu, L.-P. Li, L. Jin, Y. Bai and H. Liu, *Chem. Commun.*, 2014, **50**, 10963.
12 L. Xu, W. Ma, S. Shen, L. Li, Y. Bai and H. Liu, *Chem. Commun.*, 2016, **52**, 1162.
13 Z. Xiong, Y. Chen, L. Zhang, J. Ren, Q. Zhang, M. Ye, W. Zhang and H. Zou, *ACS Appl. Mater. Interfaces*, 2014, **6**, 22743.
14 T. E. Thingholm, O. N. Jensen, P. J. Robinson and M. R. Larsen, *Mol. Cell. Proteomics*, 2008, **7**, 661.
15 (*a*) X. Gao, H. Zhang, Q. Li, X. Yu, Z. Hong, X. Zhang, C. Liang and Z. Lin, *Angew. Chem., Int. Ed.*, 2016, **55**, 6290; (*b*) X. Huang, J. Zhang, S. Xiao and G. Chen, *J. Am. Ceram. Soc.*, 2014, **97**, 1363; (*c*) R. Wu, X. Qian, K. Zhou, J. Wei, J. Lou and P. M. Ajayan, *ACS Nano*, 2014, **8**, 6297; (*d*) Y. Liang, H. Wang, J. Zhou, Y. Li, J. Wang, T. Regier and H. Dai, *J. Am. Chem. Soc.*, 2012, **134**, 3517.
16 L. Qiu, F. Liu, L. Zhao, Y. Ma and J. Yao, *Appl. Surf. Sci.*, 2006, **252**, 4931.
17 (*a*) H. Deng, X. Li, Q. Peng, X. Wang, J. Chen and Y. Li, *Angew. Chem.*, 2005, **117**, 2842; (*b*) X.-Y. Long, Q. Song and H.-Z. Lian, *J. Mater. Chem. B*, 2015, **3**, 9330.
18 B. Sahoo, S. K. Sahu, S. Nayak, D. Dhara and P. Pramanik, *Catal. Sci. Technol.*, 2012, **2**, 1367.
19 (*a*) R. Varala, V. Narayana, S. R. Kulakarni, M. Khan, A. Alwarthan and S. F. Adil, *Arabian J. Chem.*, 2016, **9**, 550; (*b*) M. N. Alaya and M. A. Rabah, *J. Alloys Compd.*, 2013, **575**, 285.
20 (*a*) G. Cheng, J.-L. Zhang, Y.-L. Liu, D.-H. Sun and J.-Z. Ni, *Chem. Commun.*, 2011, **47**, 5732; (*b*) B. Fatima, M. Najam-ul-Haq, F. Jabeen, S. Majeed, M. N. Ashiq, S. G. Musharraf, M. A. Shad and G. Xu, *Analyst*, 2013, **138**, 5059; (*c*) Y. Zhang, L. Li, W. Ma, Y. Zhang, M. Yu, J. Guo and H. Lu, *ACS Appl. Mater. Interfaces*, 2013, **5**, 614.
21 (*a*) F. R. Rickles, R. L. Edwards, C. Barb and M. Cronlund, *Cancer*, 1983, **51**, 301; (*b*) P. Nemes, A. S. Woods and A. Vertes, *Anal. Chem.*, 2010, **82**, 982.